



MHD Oscillating Flow Of A Polar Fluid In The Presence Of Couple Stresses And Chemical Reaction

Emeka Amos* & Esien Louis Effiong

Department of Mathematics,
Rivers State University, Port Harcourt, Nigeria
*Corresponding Author: amos.emeka@ust.edu.ng

ABSTRACT

This study investigates flow of an unsteady, viscous, incompressible and electrically conducting polar fluid past a semi-infinite vertical porous plate in the presence of couple stresses and chemical reaction. The linear momentum, angular momentum, energy and concentration equations with appropriate boundary conditions as formulated in the dimensionless form are solved together by using the regular perturbation method to give approximate solutions for the flow variables. The results are displayed in plots and discussed extensively to show the effects of the variations of physical parameters found in the flow equations. It is observed that the increase in heat source, permeability of porous medium and thermal Grashof number increases the velocity of flow while the increase in chemical reaction and magnetic parameter decreases the velocity of the system. Our results also show that increase in Prandtl number decreases the temperature of the moving fluid.

Keywords: Polar fluid, couple stresses, oscillating flow, chemical reaction, MHD.

1.0 INTRODUCTION

The flow of fluids through porous media has lots of applications in several areas of human endeavors such as agricultural engineering, engineering fluid dynamics, geothermal reservoir, and geothermal energy extractions and even in the petroleum industry. The flow of polar fluids past vertical porous plates has far reaching effects in science, engineering, geophysics and even in bio- medicals. Due to the numerous applications and growing interest of scholars on the flow of polar fluids through porous media, many researchers have investigated and explored this area of fluid dynamics as evidenced by several publications. Ogulu (2005) investigated the two-dimensional flow of an electrically conducting, oscillatory, viscous polar past an infinite vertical plate whose temperature varies periodically about a mean constant non-zero value with time and solved the resulting equations by standard perturbation series method. The results obtained show that increase in radiation parameter results in a decrease in velocity, while an increase in viscous dissipation heat results to an increase in the velocity. Reddy and Shamshuddin (2016) investigated a boundary layer analysis of diffusion-thermo, heat absorption and homogenous chemical reaction on magnetohydrodynamic flow of an incompressible, laminar chemically reactive micropolar fluid past a semi-infinite vertical porous plate and numerically solved the governing equations by the finite element method. Poonian and Chaudhary (2010) investigated free convection and mass transfer flow over an infinite vertical porous plate with viscous dissipation. The governing equations in the dimensionless forms were solved analytically using two-term harmonic and non-harmonic functions and the results obtained were validated numerically. Also, Vyas and Srivastava (2010) investigated radiative MHD flow over a non-isothermal stretching sheet in a medium that is porous and converted the governing system of ordinary differential equations, by using similarity transform and then solved numerically. Furthermore, Shateyi *et al.*, (2010) investigated the influence of magnetic field on heat and mass transfer by mixed convection from vertical surfaces in the presence of Hall, radiation, Soret and Dufour effects and obtained similarity solutions using suitable transformations which are then solved by MATLAB routine `bvp4c`. Rajasekhar *et al.*, (2012) considered the effects of

variable viscosity and thermal conductivity of an unsteady two-dimensional laminar flow of a viscous incompressible electrically conducting fluid past a semi-infinite vertical plate taking into account the mass transfer and solved the transformed governing equations in the dimensionless forms analytically by using a perturbation technique. Thermophoresis effect on unsteady magnetohydrodynamic free convection flow over an inclined porous plate with time dependent suction in the presence of magnetic field and heat generation was analyzed by Kabir and Mahbub (2012). They employed the Nachtsheim-Swigert shooting iteration technique along with Sixth order Runge –Kutta integration scheme to solve the dimensionless equations modeling the problem. Vidyasagar *et al.*, (2015) investigated the two dimensional steady MHD boundary layer flow of a viscous incompressible and electrically conducting fluid over a non-isothermal linearly stretching sheet that is embedded in a fluid saturated porous medium with the effect of radiation and solved the governing system of partial differential equations by shooting method. Their result shows that the velocity profile increases with an increase in Grashof of number. The influence of thermal radiation on some unsteady MHD free convection flows of an incompressible Brinkman type fluid past a vertical flat plate embedded in a porous medium with Newtonian heating boundary condition was analyzed by Ali *et al.*, (2013). They tackled the transformed dimensionless governing equations analytically using Laplace transform technique. Amos and Israel-Cookey (2016) studied the Soret and magnetic effects on the onset of convection in a shallow horizontal porous layer with thermal radiation and obtained the solutions to the problem analytically and numerically. Furthermore, Bhadauria (2016) investigated the chaotic convection in a viscoelastic fluid saturated porous layer, heated from below by using Oldroyd's type constituting relation and in the presence of an internal heat source and solved the problem by constructing an autonomous system of fourth-order differential equations using a truncated Fourier series.

Krishnamurthy *et al.* (2016) studied the effects of radiation and chemical reaction on the unsteady boundary layer flow of MHD Williamson fluid through porous medium towards a horizontal linearly stretching sheet in the presence of nano particles and the resultant dimensionless equations describing the problem are solved numerically by the Runge-Kutta Fehlberg fourth-fifth order method with shooting technique. Vieru *et al.* (2015) investigated the time-fractional free convection flow of an incompressible viscous fluid near a vertical plate with Newtonian heating and mass diffusion in the presence of first order chemical reaction and solved the dimensionless equations governing the problem by the Laplace transform technique. Reddy *et al.* (2015) investigated the effect of chemical reaction on an unsteady free convection flow past a semi-infinite vertical plate with viscous dissipation and analyzed the governing equations of motion, energy and species concentration analytically by the regular perturbation technique.

Uwanta *et al.* (2014) considered an unsteady hydro-magnetic free convective flow of a viscous, incompressible, electrically conducting, and heat radiating fluid past a flat plate with ramped wall temperature and suction/blowing and subjected the governing equations to Laplace transformation followed by numerical inversion using INVLAP routine of MATLAB. Unsteady magnetohydrodynamic free convective, visco-elastic, dissipative fluid flow embedded in porous medium bounded by an infinite inclined porous plate in the presence of heat source and Ohmic heating under the influence of transversely applied magnetic field of uniform strength was studied by Umamaheswar *et al.* (2013). Solutions to the governing equations were presented using a multiple parameter perturbation technique subject to the relevant boundary convections. Khan *et al* (2014) observed the effect of wall shear stress on MHD conjugate flow over an inclined plate in a porous medium with ramped wall temperature and solved the resulting equations governing the flow by using the Laplace transform technique. Sivaiah and Reddy (2017) investigated the effects of Hall current and radiation on MHD free convective heat and mass transfer flow of a radiative fluid past an accelerated inclined porous plate in the presence of thermal radiation and heat source and solved the governing equations for the velocity, temperature and concentration distributions by the Laplace transfer technique.

Investigation of magnetohydrodynamics (MHD) oscillating flow of a chemically reactive, viscous and electrically conducting polar fluid with coupled stresses is the subject of this investigation.

2. MATHEMATIAL FORMULATIONS

We consider the flow of an unsteady, viscous, incompressible, chemically reactive and electrically conducting polar fluid through a porous medium past a semi-infinite vertical plate in which the x – axis is taken along the vertical plate in the fluid flow direction and the y – axis is normal to it.

Here, we assume that the plate is long enough in the x –direction so that the physical variables describing the fluid flow are functions of y and t only, and that there is a first order chemical reaction between diffusing species. Also, the induced magnetic field is neglected and we apply magnetic field of intensity H_0 perpendicular to the plate. Under the above simplifying assumptions, the governing equations for the flow are:

$$\frac{\partial u'}{\partial y'} = 0 \tag{1}$$

$$\frac{\partial u'}{\partial t'} + v' \frac{\partial u'}{\partial y'} = (v + v_r) \frac{\partial^2 u'}{\partial y'^2} + 2v_r \frac{\partial u'}{\partial y'} - \frac{\nu}{K'} u' - \frac{\sigma \mu^2 H_0^2}{\rho} u' + g \beta_T (T' - T'_\infty) + g \beta_c (C' - C'_\infty) \tag{2}$$

$$\frac{\partial \Omega'}{\partial t'} + v' \frac{\partial \Omega'}{\partial y'} = \frac{\gamma^*}{I} \frac{\partial^2 \Omega'}{\partial y'^2} \tag{3}$$

$$\frac{\partial T'}{\partial t'} + v' \frac{\partial T'}{\partial y'} = \xi \frac{\partial^2 T'}{\partial y'^2} - \xi \frac{\partial q_r'}{\partial y'} - \frac{Q_0}{\rho c_p} (T' - T'_\infty) \tag{4}$$

$$\frac{\partial C'}{\partial t'} + v' \frac{\partial C'}{\partial y'} = D \frac{\partial^2 C'}{\partial y'^2} - k_r^* (C' - C'_\infty) \tag{5}$$

The boundary conditions for the governing equations are

$$u' = 0, T' = T'_w + \varepsilon(T' - T'_\infty)e^{i\omega t}, \frac{\partial \Omega'}{\partial y'} = u'_p, C' = C'_w + \varepsilon(C' - C'_\infty)e^{i\omega t} \quad \text{at } y' = 0 \tag{6}$$

$$u' \rightarrow 0, T' \rightarrow T'_\infty, C' \rightarrow C'_\infty, \Omega' \rightarrow 0 \quad \text{as } y' \rightarrow \infty \tag{7}$$

where u' and v' are components of velocity in the x' and y' directions respectively, g is the acceleration due to gravity, β_T and β_c are the coefficients of volume expansion due to temperature and concentration respectively, t' is time, ρ is the density, D is the molecular diffusivity, H_0 is magnetic field, q_r is radiation flux, K' is the permeability of the porous medium, v_r is the rotational coefficient of kinematic viscosity, ν kinematic viscosity, k_r^* is chemical reaction, I is a scalar constant, Q_0 heat source parameter, ξ is thermal diffusivity, T' is dimensional temperature, C' is dimensional concentration, Ω' is angular velocity component.

The velocity depends on time as

$$v' = -v_o(1 + \varepsilon Ae^{i\omega t}) \tag{8}$$

where A is a real positive constant such that $\varepsilon A \ll 1$, v_o is a scalar known as suction velocity which is usually a non-zero positive constant.

To write the governing equations and the boundary conditions in the dimensionless form, the following non- dimensional variables are introduced;

$$y = \frac{V_o y'}{v}; u = \frac{u'}{V_o}; \omega' = \frac{V_o^2}{v}; t = \frac{v_o^2 t'}{v}; \Omega = \frac{\Omega' v}{V_o^2}; \theta = \frac{T' - T_\infty}{T_w - T_\infty}; C = \frac{C' - C_\infty}{C_w - C_\infty};$$

$$k = \frac{K' v_o^2}{v^2}; t = \frac{t' v_o^2}{v}; \alpha = \frac{v_r}{v}; \beta^* = \frac{1v}{v}; K_r = \frac{K_r' v}{v_o^2}; Sc = \frac{v}{D}; u_p = \frac{v_o^3 u'_p}{v^2} \tag{9}$$

Introducing the Roseland diffusion approximation for the radiative heat flux in equation (4), that is

$$q_r' = -\frac{4\sigma^* \partial T'^4}{3K^* \partial y'} \tag{10}$$

where σ^* is the Stefan-Boltzmann constant and K^* is the Roseland mean absorption coefficient. If we assume that the temperature difference between the fluid and the flow boundaries is sufficiently small then we can express T'^4 in Taylors series as a linear combination of the temperature about the free stream temperature T'_∞ and by neglecting higher order terms, we have

$$T'^4 \approx -3T_\infty'^4 + 4T_\infty'^3 T' \tag{11}$$

Hence

$$\frac{\partial q_r'}{\partial y'} = -\frac{16\sigma^* k T_\infty'^3}{3\rho c_p k^*} \frac{\partial^2 T'}{\partial y'^2} \tag{12}$$

Equation (4) therefore becomes

$$\frac{\partial T'}{\partial t'} + v' \frac{\partial T'}{\partial y'} = \xi \frac{\partial^2 T'}{\partial y'^2} - \xi \frac{16\sigma^* k T_\infty'^3}{3\rho c_p k^*} \frac{\partial^2 T'}{\partial y'^2} + \frac{Q_o}{\rho c_p} (T' - T_\infty') \tag{13}$$

Using the non-dimensional variables in Equation (9) to rewrite Equations (2, 3, 5, 6, 7,13), the governing equations describing the flow of the fluid together with the boundary conditions in the dimensionless form are summarized thus:

$$\frac{\partial u}{\partial t} - (1 + \varepsilon Ae^{i\omega t}) \frac{\partial u}{\partial y} = (1 + \alpha) \frac{\partial^2 u}{\partial y^2} + 2\alpha \frac{\partial \Omega}{\partial y} - \left(\frac{1}{K} + M\right) u + G_r \theta + G_c c \tag{14}$$

$$\frac{\partial \Omega}{\partial t} - (1 + \varepsilon Ae^{i\omega t}) \frac{\partial \Omega}{\partial y} = \frac{1}{\beta^*} \frac{\partial^2 \Omega}{\partial y^2} \tag{15}$$

$$\frac{\partial \theta}{\partial t} - (1 + \varepsilon Ae^{i\omega t}) \frac{\partial \theta}{\partial y} = \frac{(1 + R_\theta)}{Pr} \frac{\partial^2 \theta}{\partial y^2} + Hs\theta \tag{16}$$

$$\frac{\partial c}{\partial t} - (1 + \varepsilon Ae^{i\omega t}) \frac{\partial c}{\partial y} = \frac{1}{Sc} \frac{\partial^2 c}{\partial y^2} - k_r c \tag{17}$$

With boundary Conditions:

$$u = 0 ; \theta = 1 + \varepsilon e^{i\omega t}; \frac{\partial \Omega}{\partial y} = u_p ; C = 1 + \varepsilon e^{i\omega t} \quad \text{for } y = 0: \quad (18)$$

$$u = 0, \theta \rightarrow 0, C \rightarrow 0, \Omega \rightarrow 0 \quad \text{as } y \rightarrow \infty: \quad (19)$$

The flow parameters entering the problem are:

$$M = \frac{\sigma \mu^2 H_0^2 u}{\rho \nu_0^2} ; G_r = \frac{g \beta T u (T'_w - T'_{\infty})}{\nu_0^3} ; G_c = \frac{g \beta_c u (c'_w - c'_{\infty})}{\nu_0^3} ; H_s = \frac{Q_0 \nu}{\rho c_p \nu_0^2} , Pr = \frac{\rho c_p \nu}{k} = \frac{\nu}{\xi}$$

$$R_a = \frac{16 \delta^* T_{\infty}^3}{3k^* (T'_{\omega} - T'_{\infty})} , Sc = \frac{\nu}{D} \quad (20)$$

represented respectively as magnetic field, thermal Grashof number, solutal Grashof number, heat source, Prandtl number, Radiation parameter, and Schmidt number.

3. METHOD OF SOLUTION

To find the analytical solutions of the coupled nonlinear partial differential equations (14)-(17) together with the boundary conditions equations (18) and (19), are solved using the Regular Perturbation Method by expanding the velocity u , temperature θ , concentration C and angular momentum Ω of the fluid in the neighborhood of the plate as follows:

$$u(y, t) = u_0(y) + \varepsilon e^{i\omega t} u_1 + 0(\varepsilon^2) \quad (21)$$

$$\Omega(y, t) = \Omega_0(y) + \varepsilon e^{i\omega t} \Omega_1 + 0(\varepsilon^2) \quad (22)$$

$$\theta(y, t) = \theta_0(y) + \varepsilon e^{i\omega t} \theta_1 + 0(\varepsilon^2) \quad (23)$$

$$C(y, t) = C_0(y) + \varepsilon e^{i\omega t} C_1 + 0(\varepsilon^2) \quad (24)$$

Consequently the following equations are obtained

$$(1 + \alpha)u_0'' + u_0' - Nu_0 = -2 \alpha \Omega_0' - G_r \theta_0 - G_c C_0 \quad (25)$$

$$(1 + \alpha)u_1'' + u_1' - (J + N)u_1 = -Au_0' - 2 \alpha \Omega_1' - G_r \theta_1 - G_c C_1 \quad (26)$$

$$\Omega_0'' + \beta^* \Omega_0' = 0 \quad (27)$$

$$\Omega_1'' + \beta^* \Omega_1' - i\omega \beta^* \Omega_1 = -A\beta^* \Omega_0' \quad (28)$$

$$(1 + R_a)\theta_0'' - Pr\theta_0' + Pr H_s \theta_0 = 0 \quad (29)$$

$$(1 + R_a)\theta_1'' - Pr\theta_1' + Pr(H_s - i\omega)\theta_1 = -AP_r\theta_0' \quad (30)$$

$$C_0'' + Sc C_0' - Sc k_r C_0 = 0 \tag{31}$$

$$C_1'' + Sc C_1' - Sc(i\omega + k_r)C_1 = -AScC_0' \tag{32}$$

The perturbed boundary conditions are

$$u_0 = 0; u_1 = 0, \theta_0 = 1; \theta_1 = 1, \Omega_0' = u_\rho; \Omega_1' = u_\rho, C_0 = 1; C_1 = 1: \text{for } y = 0 \tag{33}$$

$$u_0 \rightarrow 0; u_1 \rightarrow 0, \theta_0 \rightarrow 0; \theta_1 \rightarrow 0, C_0 \rightarrow 0; C_1 \rightarrow 0, C_0 \rightarrow 0; C_1 \rightarrow 0, \Omega_0 \rightarrow 0; \Omega_1 \rightarrow 0: \text{as } y \rightarrow \infty \tag{34}$$

where, $N = \left(\frac{1+kM}{k}\right), (J+N) = \left(\frac{i\omega k+kM+1}{k}\right)$

The solutions to Equations (25)-(32) subject to (33) to (34) are presented as follows

$$C(y, t) = e^{z_1 y} + \varepsilon e^{i\omega t} (D_1 e^{z_2 y} - B e^{z_1 y}) \tag{35}$$

$$\theta(y, t) = e^{z_3 y} + \varepsilon e^{i\omega t} (D_5 e^{z_4 y} - B_2 e^{z_3 y}) \tag{36}$$

$$\Omega(y, t) = \frac{u_\rho}{\beta^*} e^{\beta^* y} + \varepsilon e^{i\omega t} \left(\frac{-B_5 \beta^*}{z_5} e^{z_5 y} + B_3 e^{\beta^* y} \right) \tag{37}$$

$$u(y, t) = D_{11} e^{z_6 y} - B_4 e^{\beta^* y} - B_5 e^{z_3 y} - B_6 e^{z_1 y} + \varepsilon e^{i\omega t} (-B_7 e^{\beta^* y} + B_8 e^{z_1 y} - B_9 e^{z_2 y} + B_{10} e^{z_3 y} - B_{11} e^{z_4 y} + B_{12} e^{z_5 y} - B_{13} e^{z_6 y} + D_{13} e^{z_7 y}) \tag{38}$$

The skin friction τ , heat transfer Nu , and mass transfer Sh are given respectively as

$$\tau = \left. \frac{\partial u}{\partial y} \right|_{y=0} \tag{39}$$

$$Nu = \left. \frac{\partial \theta}{\partial y} \right|_{y=0} \tag{40}$$

$$Sh = \left. \frac{\partial C}{\partial y} \right|_{y=0} \tag{41}$$

4. DISCUSSION OF RESULTS

Our computation have shown that the parameters under investigation are magnetic field ‘M’, Schmidt number Sc , Heat Source HS , thermal Radiation Ra , Chemical reaction Kr , Permeability K , Thermal Grashof number Gr , Solutal Grashof number Gc , Prandtl number Pr . These parameters influences convective heat and Mass transfer and are therefore, illustrated in figures and discussed below.

Figure 1 shows the influence of Schmidt number on the Velocity distribution. It is observed that at low value ($Sc = 0.1$) of the Schmidt number, the peak of the velocity profiles is highest and decreases as the Schmidt number values are increased. Physically, this is as a result of decrease in the momentum boundary layer due to the increase in Schmidt number, hence a decrease in the velocity of the fluid. Figure 2 illustrates the influence of magnetic field on the velocity distribution. The profile shows that

increase in the magnetic field decreases the velocity of the fluid. Physically, we know that in the motion of an electrically conducting fluid in the presence of applied magnetic field, the Lorentz force is generated in the flow field. The Lorentz force has the tendency to retard fluid velocity and this is confirmed in this study as shown in the plot. This finding agrees with the study of Umamheswar *et al* (2016). Our computation shows that at very high magnetic field values, the flow is retarded significantly. The effect of the thermal Grashof number and the solutal Grashof number is shown in figures 3 and 4 and they represent the thermal buoyancy force and solutal buoyancy force respectively. Both show increase in velocity as the Grashof numbers are increased. Physically, the increase in the buoyancy force increases the boundary layer thickness and therefore, enhances the velocity of the fluid. A close observation shows that the maximum and minimum peaks are higher in the solutal Grashof number than in the thermal Grashof number indicating that the solutal buoyancy force exerts more influence in the flow.

Figure 5 shows the influence of heat source on the velocity field. It is observed that the case of heat generation in the system increases the velocity of the fluid. Physically, this is due to increase in the buoyancy force, due to increase in the heat generation. The response of velocity distribution due to variation in the thermal radiation is shown in figure 6. Increase in the thermal radiation increases the velocity. Figure 7 shows the influence of chemical reaction on the velocity field. The increment in the chemical reaction parameter reduces the flow. The effect is more pronounced near the plate where the profiles assume maximum peak and then decelerate to the free stream velocity outside the boundary layer. This agrees with Pal and Talukdar (2010). The influence of permeability of the porous medium on the flow is shown in figure 8. Increase in the permeability increases the velocity of the fluid as more fluid flows when the porosity of the medium is increased.

The variation of the fluid temperature under the influence of the Prandtl number is shown in figure 9. The profiles indicate a decrease in the fluid temperature due to increase in the Prandtl number. If the Prandtl number is small, there is an increase in the thermal conductivity of the fluid. Also for smaller values of Prandtl number, the thermal boundary layer is thicker; leading to increase in the temperature profile, but higher values of the Prandtl number decreases the temperature. Figure 10 illustrates temperature distribution due to the effect of thermal radiation. The temperature is enhanced by increase in the thermal radiation. Physically increment in thermal radiation means further diffusion of energy. Figure 11 displays effect of chemical reaction on the concentration distribution. The profile indicates that increase in chemical reaction decreases the concentration of species in the boundary layer. Physically, this is because the solutal boundary layer thickness for chemical reaction is been reduced. This also confirms that diffusion rates can be tremendously altered by chemical reaction.

The influence of the Schmidt number on the concentration distribution is displayed in figure 12, it is observed that there is a reduction in the concentration due to decrease in the value of the Schmidt number. Physically increase in the Schmidt means decrease in molecular diffusion. This therefore ensures higher concentration of species for small Schmidt number and vice versa. This agrees with Pal and Talukdar (2010). Figure 13 shows the effect of the real positive constant on the micro rotation. It is observed that increase in the positive constant decreases the micro rotation. The influence of frequency of oscillation in micro rotation is shown in figure 14. Increase in the frequency of oscillation decreases the micro rotation.

Figure 15 shows the effect of thermal radiation and Heat source, on heat transfer rate. It is revealed from the profile that increase in thermal radiation leads to, first, a reduction in heat transfer rate and then an increase in heat transfer especially with further increase in the heat generation at which point we observe a linear relationship between the heat transfer rate and heat generation. The simultaneous effect of the chemical reaction and Schmidt number is shown in figure 16. A linear relationship is observed in the mass transfer on increase in both chemical reaction and Schmidt number. Figure 17 shows the effect of Schmidt number and chemical reaction on the skin friction. Increase in Schmidt number decreases the skin friction with further increase in the chemical reaction decreasing the skin friction more. This is an indication that the skin friction is higher at lower values of the chemical reaction. Figure 18 shows the influence of thermal Grashof number and Permeability on the skin friction. The profiles indicate that the skin friction increases with increase in the thermal Buoyancy force and rises initially (at very low values

of the permeability. At $K = 1$, the skin friction is constant irrespective of the increase in the value of the permeability of the medium.

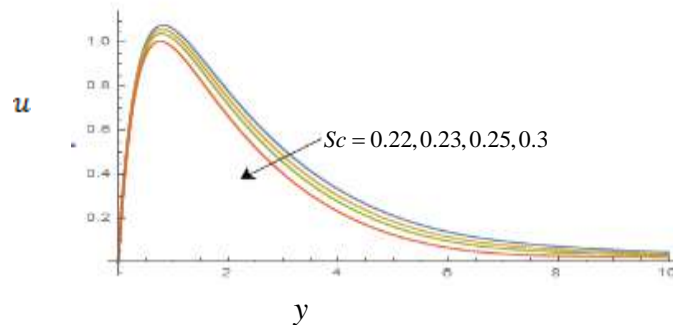


Fig 1: Effect of Schmidt Number on Velocity Distribution for $Kr = 0.5$, $\omega = 0.1$, $Ra = 2$, $Hs = 2$, $\alpha = 0.2$, $Gr = 2$, $Pr = 0.71$, $Gc = 2$, $u_p = 1$, $\beta^* = 1$, $\varepsilon = 0.2$, $J = 0.1$, $t = 1$, $M = 0.5$, $K = 0.2$

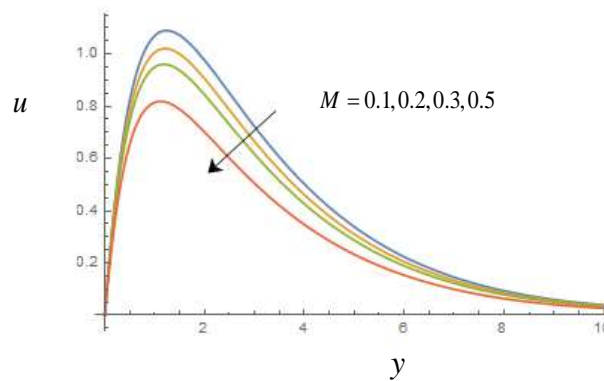


Fig 2: Effect of Magnetic Parameter on Velocity Distribution for $Sc = 0.22$, $\omega = 0.1$, $Pr = 0.71$, $Ra = 2$, $Hs = 2$, $Kr = 0.5$, $\alpha = 0.2$, $Gr = 2$, $Gc = 2$, $u_p = 1$, $\beta^* = 1$, $\varepsilon = 0.2$, $t = 1$, $K = 0.2$

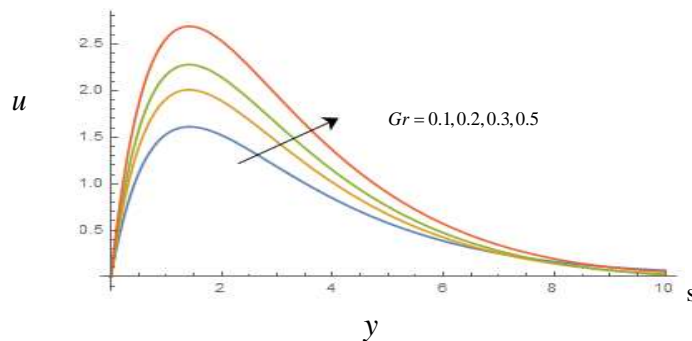


Fig 3: Effect of Thermal Grashof Number on Velocity Distribution for $Sc = 0.22$, $\omega = 0.1$, $Pr = 0.71$, $Ra = 2$, $Hs = 2$, $Kr = 0.5$, $\alpha = 0.2$, $Gc = 2$, $u_p = 1$, $\beta^* = 1$, $\varepsilon = 0.2$, $t = 1$, $M = 0.5$, $K = 0.2$

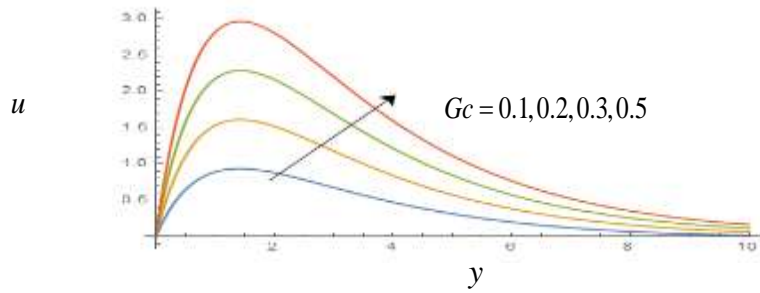


Fig 4: Effect of Solutal Grashof Number on Velocity Distribution for $Sc = 0.22, \omega = 0.1, Pr = 0.71, Ra = 2, Kr = 0.5, Hs = 2, \alpha = 0.2, Gr = 2, u_p = 1, \beta^* = 1, \epsilon = 0.2, t = 1, M = 0.5, K = 0.2$

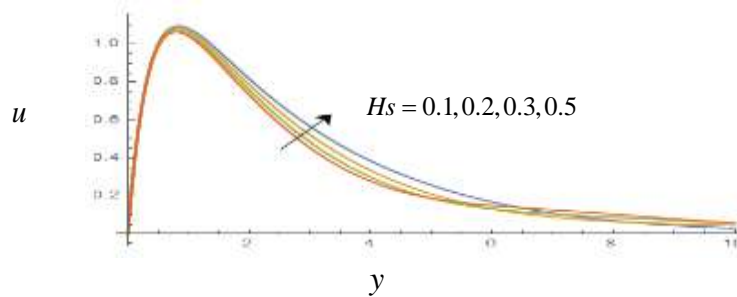


Fig 5: Effect of Heat Source on Velocity Distribution for $Sc = 0.22, \omega = 0.1, Pr = 0.71, Ra = 2, \alpha = 0.2, Kr = 0.5, Gr = 2, Gc = 2, u_p = 1, \beta^* = 1, \epsilon = 0.2, t = 1, M = 0.5, K = 0.2$

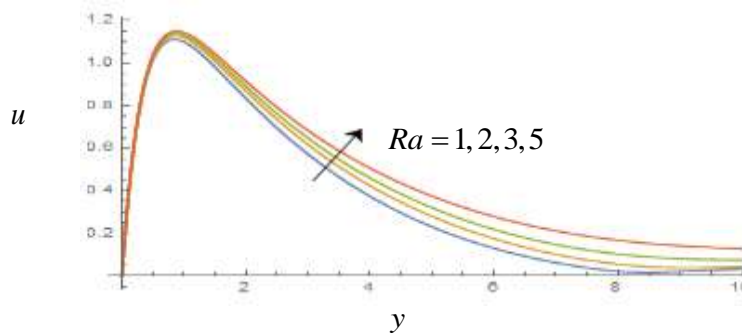


Fig 6: Effect of Radiation on Velocity Distribution for $Sc = 0.22, \omega = 0.1, Pr = 0.71, Hs = 2, Kr = 0.5, \alpha = 0.2, Gr = 2, Gc = 2, u_p = 1, \beta^* = 1, \epsilon = 0.2, t = 1, M = 0.5, K = 0.2$

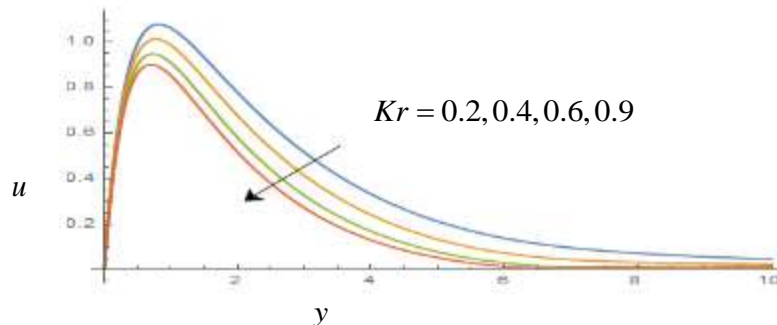


Fig 7: Effect of Chemical Reaction on Velocity Distribution for $Sc = 0.22, \omega = 0.1, Ra = 2, Hs = 2, Pr = 0.71, \alpha = 0.2, Gr = 2, Gc = 2, u_p = 1, \beta^* = 1, \varepsilon = 0.2, t = 1, M = 0.5, K = 0.2$

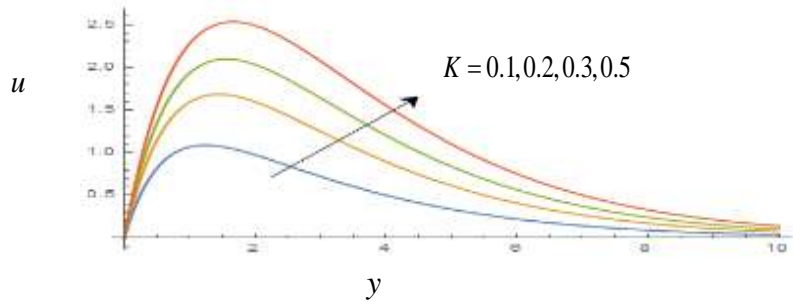


Fig 8: Effect of Permeability on Velocity Distribution for $Sc = 0.22, \omega = 0.1, Pr = 0.71, Ra = 2, Hs = 2, Kr = 0.5, \alpha = 0.2, Gr = 2, Gc = 2, u_p = 1, \beta^* = 1, \varepsilon = 0.2, t = 1, M = 0.5$

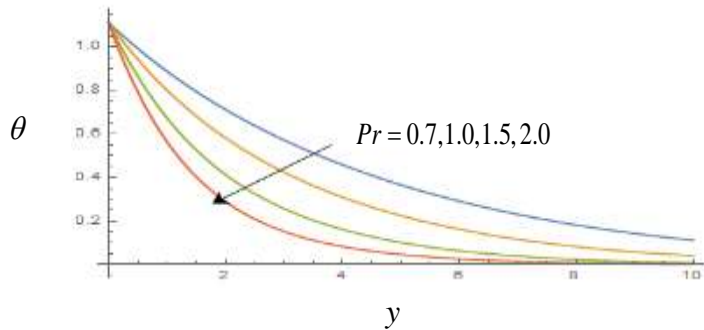


Fig 9: Effect of Prandtl Number on Temperature Distribution for $Hs = 2, Ra = 2, \omega = 0.1, A = 1, \varepsilon = 0.2, t = 1$

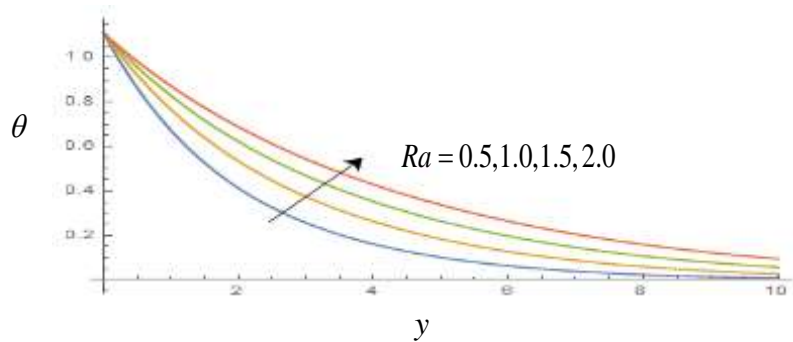


Fig 10: Effect of Thermal Radiation on Temperature distribution for $Hs = 2, Pr = 0.71, \omega = 0.1, A = 1, \varepsilon = 0.2, t = 1$

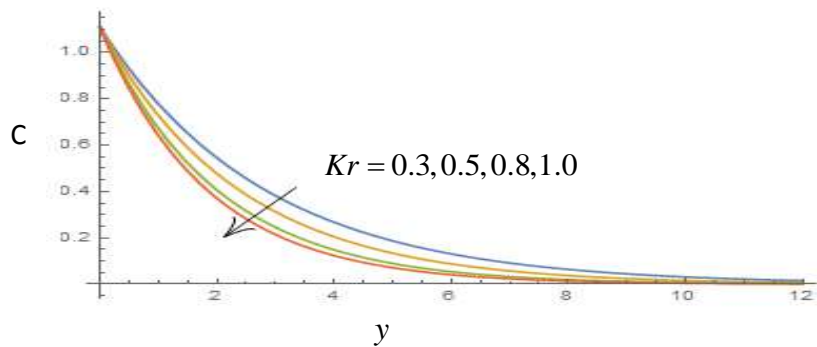


Fig 11: Effect of Chemical reaction on Concentration distribution for $Sc = 0.22, \omega = 0.1, \varepsilon = 0.2, A = 1, t = 1$

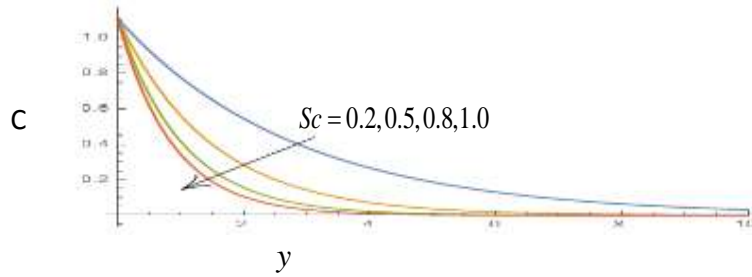


Fig 12: Effect of Schmidt Number on Concentration Distribution for $Kr = 0.5, \omega = 0.1, \varepsilon = 0.2, A = 1, t = 1$

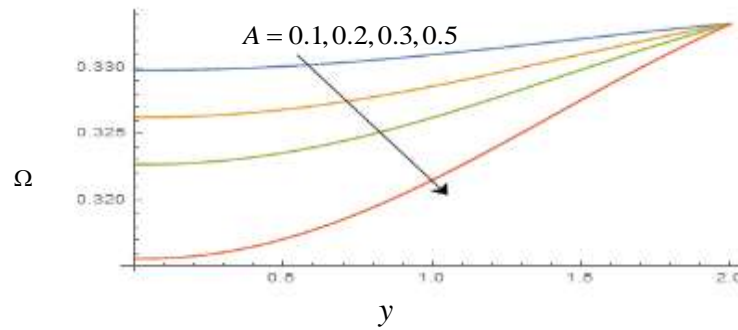


Fig 13: Effect of Positive constant on Micro Rotation for $u_p = 1, \beta^* = 1, A = 1, \varepsilon = 0.2, t = 1$

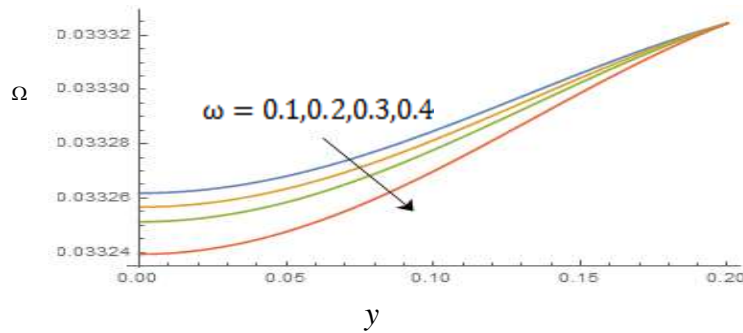


Fig 14: Effect of Oscillation on Micro Rotation for $u_p = 1, \beta^* = 1, A = 1, \varepsilon = 0.2, t = 1$

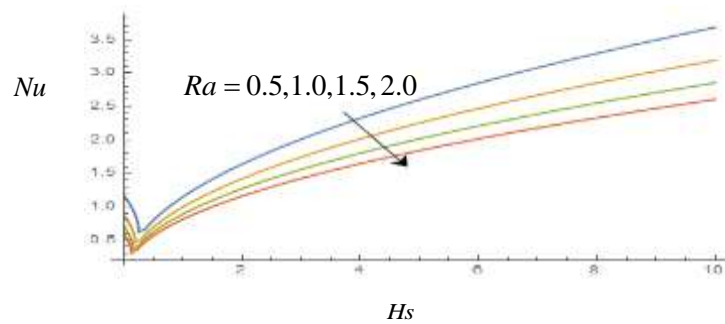


Fig 15: Effect of Thermal Radiation and Heat Source on Heat Transfer for : $Sc = 0.22, \omega = 0.1, Pr = 0.71, Kr = 0.5, \alpha = 0.2, Gr = 2, Gc = 2, u_p = 1, \beta^* = 1, \varepsilon = 0.2, t = 1$

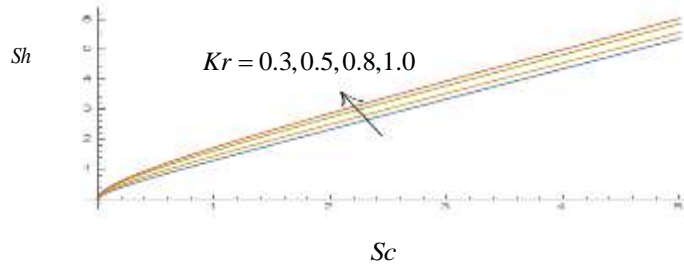


Fig 16: Effect of Chemical Reaction and Schmidt Number on Mass Transfer for: $Kr = 0.5, \omega = 0.1, \varepsilon = 0.2, A = 1, t = 1$

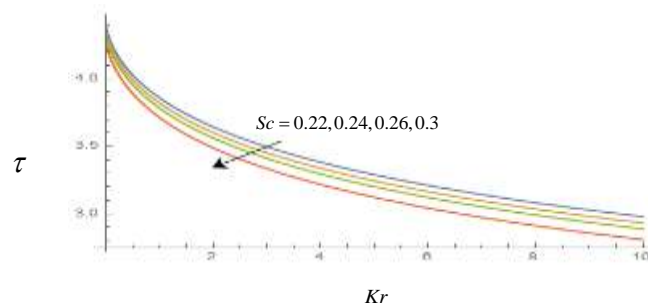


Fig 17: Effect of Schmidt Number and Chemical Reaction on Skin Friction for $= 2, n = 0.1, Pr = 0.71, Ra = 2, \alpha = 0.2, Gr = 2, Gc = 2, u_p = 1, \beta^* = 1, \varepsilon = 0.2, t = 1$

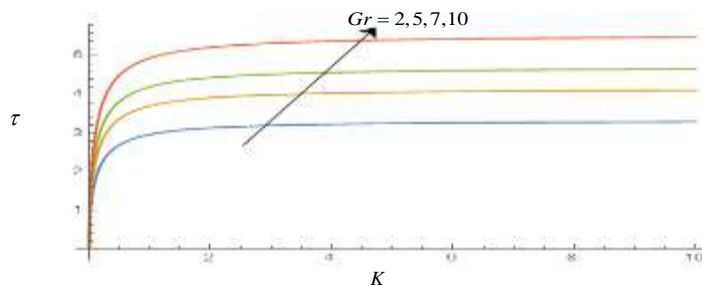


Fig 18: Effect of Grashof Number and Permeability on Skin Friction for: $Hs = 2, \omega = 0.1, Pr = 0.71, Ra = 2, \alpha = 0.2, Gc = 2, u_p = 1, \beta^* = 1, \varepsilon = 0.2, t = 1, M = 0.5, Kr = 0.5$

5. CONCLUSIONS

This study analyzed MHD oscillatory flow of a polar fluid in the presence of couple stresses and chemical reaction. The computations show that the parameter under investigation are magnetic field M , Schmidt number Sc , Heat Source Hs , thermal Radiation Ra , Chemical reaction Kr , Permeability K , thermal Grashof number Gr , Solutal Grashof number Gc , Prandtl number Pr . The results and graphical displays shows the behavior and nature of the problem for velocity, energy, concentration and angular momentum. It is seen that the velocity field increases when there is an increase in the heat generated in the system. It

also reveals that increase in Schmidt number decreases the skin friction with further increase in the chemical reaction decreasing the skin friction more. Also increase in the Schmidt number physically means a decrease in molecular diffusion, which ensures higher species concentration for small Schmidt number and vice-versa. The results also show that an increase in the frequency of oscillation decreases the micro rotation. Also increase in the thermal Grashof number increases the velocity of the fluid.

REFERENCES

- Ali, F., Khan, I., Shafie, S. & Musthapa, N. (2013). Heat and mass transfer with free convection MHD flow past a vertical plate embedded in a porous medium. *Mathematical Problems in Engineering*, 346281, 1
- Amos, E. & Israel-Cookey, C. (2016). Soret and magnetic effects on the onset of convection in a shallow horizontal porous layer with thermal radiation. *International Journal of Engineering and Applied Sciences*, 8(2).10-18.
- Bhadauria, B. S. (2016). Chaotic convection in a viscoelastic fluid saturated porous medium with a heat source. *Journal of Applied Mathematics*, 1487618, 1 - 18
- Das, M., Mahato, R. & Nandkeolyar, R. (2015). Newtonian heating effect on unsteady hydromagnetic Casson fluid flow pass a flat plate with heat and mass transfer. *Alexandria Engineering Journal*, 54(4), 871-879.
- Kabir, M. A. & AlMahbub, M. A. (2012). Effects of Thermophoresis on unsteady MHD free convective heat and mass transfer along an inclined porous plate with heat generation in presence of magnetic field. *Open Journal of Fluid Dynamics*, 2(4), 120.
- Khan, A., Khan, I., Ali, F & Shafie, S. (2014). Effects of wall shear stress on MHD conjugate flow over an inclined plate in a porous medium with ramped wall temperature. *Mathematical Problems in Engineering*, 861708, 1 – 15.
- Krishnamurthy.M.R, Prasannakumara, B.C. Gireshe, B. J., Rama, S. & Reddy, G (2016). Effect of Chemical reaction on MHD boundary Williamson nano-fluid in porous medium. *Engineering Science and Technology an International Journal*, 1(9), 53-61
- Uwanta, I. J., & Hamza, M. M. (2014). Effect of suction/injection on unsteady hydromagnetic convective flow of reactive viscous fluid between vertical porous plates with thermal diffusion. *International scholarly research notices*, 980270, 1 - 14.
- Ogulu, A. (2005). On the oscillating plate-temperature flow of a polar fluid past a vertical porous plate in the presence of couple stresses and radiation. *International Communications in Heat and Mass Transfer*, 32(9), 1231-1243.
- Pal D. and Talukdar B. (2010). Perturbation analysis of unsteady magnetohydrodynamic convective heat and mass transfer in a boundary layer slip flow past a vertical permeable plate with thermal radiation and chemical reaction. *Commun Nonlinear Sci Numer Simulat*, 15, 1813 – 1830.
- Poonian, H & Chaudhary, R. C. (2010). MHD free convection and mass transfer flow over an infinite vertical porous plate with viscous dissipation. *Theoretical and Applied Mechanics*, 37(4), 263-287.
- Rajasekhar, K., Reddy, G. R & Prasad, B. D. C. N. (2012). Unsteady MHD free convective flow past a semi-infinite vertical porous plate. *Energy Conservation*, 2(2), 2.
- Reddy, A. N., Vidya, S., Raju, M., C., & Vagma, S. V. K., (2015). Thermal and solution Buoyancy Effect on Viscous Dissipative and chemically Reactive Fluid flow past a uniformly moving plate with valuable Suction *International Journal of Innovative Technology and Exploring Engineering*, 5(7), 2278- 3075.
- Shateyi, S., Motsa, S. S & Sibanda, P. (2010). The effects of thermal radiation, hall currents, Soret, and Dufour on MHD flow by mixed convection over a vertical surface in porous media. *Mathematical Problems in Engineering*, 6274751, 1.
- Shamshuddin, M. D., Béq, O. A., Reddy, S. S., & Kadir, A. (2018). Rotating unsteady multi-physico-chemical magneto-micropolar transport in porous media: Galerkin finite element study. *Computational Thermal Sciences: An International Journal*, 10(2).

- Sivaiah, G., & Reddy, K. J. (2016). Unsteady MHD heat and mass transfer flow of a Radiating fluid past an Accelerated inclined porous plate with hall current. *International Journal of Research*, 5(7), 2394-3629.
- Umamheswar, M., Varma, S.V.K & Raju M.C (2016). Numerical study of magnetic- convective and radiation absorption fluid flow past an exponentially accelerated vertical porous plate with variable temperature and in the presence of Soret and Dufour effects. *Journal of Mathematics*, 12(2), 109-120.
- Vidyasagar, B., Raju, M. C & Varma, S. V. K. (2015). Unsteady MHD Free Convection Flow of a Viscous Dissipative Kuvshinski Fluid Past an Infinite Vertical Porous Plate in the Presence of Radiation, Thermal Diffusion and Chemical Effects. *Journal of Applied and Computational Mathematics*, 4(255), 2.
- Vieru, D., Fetecau, C & Fetecau, C. (2015). Time-Fractional Free Convection Flow Near a Vertical Plate With Newtonian Heating and Mass Diffusion. *Thermal Science*, 19(1), 85 – 98.
- Vyas, P & Srivastava, N. (2010). Rachative MHD flow over a non-Isothermal stretching sheet in a Porous medium. *Applied Mathematical Sciences*, 4(49-52), 2475-2484.

APPENDIX

$$M = \frac{\sigma \mu^2 H_0^2 \nu}{\rho \nu_0^2}, \quad G_r = \frac{g \beta_T \nu (T_{\infty}^i - T_{\infty}^j)}{\nu_0^3}, \quad G_c = \frac{g \beta_C \nu (c_{\infty}^i - c_{\infty}^j)}{\nu_0^3}, \quad \alpha = \frac{\nu_r}{\nu}, \quad H_s = \frac{Q \nu}{\rho c_p \nu_0^2}, \quad N = \left(\frac{1+kM}{k} \right), \quad Sc = \frac{\nu}{D},$$

$$K_r = \frac{K_r^* \nu}{\nu_0^2}, \quad (J + N) = \left(\frac{\omega k + kM + 1}{k} \right), \quad z_1 = - \left(\frac{Sc + \sqrt{Sc^2 + 4Sc k_r}}{2} \right), \quad z_2 = - \left(\frac{Sc + \sqrt{Sc^2 + 4Sc (n+k_r)}}{2} \right)$$

$$B = \frac{-ASc z_1}{z_1^2 + Sc z_1 - Sc (i\omega + k_r)}, \quad z_3 = - \left(\frac{Pr + \sqrt{Pr^2 - 4Pr H_s (1+R_B)}}{2(1+R_B)} \right), \quad D_5 = 1 + \frac{AP_r z_3}{(1+R_B) z_3^2 - Pr z_3 + Pr (H_s - n)}$$

$$z_4 = - \left(\frac{Pr + \sqrt{Pr^2 - 4Pr (1+R_B) (H_s - i\omega)}}{2(1+R_B)} \right), \quad B_2 = \frac{-AP_r z_3}{(1+R_B) z_3^2 - Pr z_3 + Pr (H_s - i\omega)}, \quad z_5 = e^{- \left(\frac{\beta^* + \sqrt{\beta^{*2} + 4i\omega \beta^*}}{2} \right)}, \quad B_3 = \frac{-Au\rho}{2\beta^* - i\omega}$$

$$D_7 = \frac{-B_3 \beta^*}{z_5}, \quad B_4 = \frac{-2\alpha u \rho}{(1+\alpha)\beta^{*2} + \beta^* - N}, \quad B_5 = \frac{-G_r}{(1+\alpha)z_1^2 + z_1 - N}, \quad B_6 = \frac{-G_c}{(1+\alpha)z_2^2 + z_2 - N}, \quad z_6 = - \left(\frac{1 + \sqrt{1 + 4N(1+\alpha)}}{2(1+\alpha)} \right)$$

$$D_{11} = \frac{2\alpha u \rho \beta^*}{(1+\alpha)\beta^{*2} + \beta^* - N} + \frac{G_r}{[(1+\alpha)z_1^2 + z_1 - N]} + \frac{G_c}{[(1+\alpha)z_2^2 + z_2 - N]}, \quad z_7 = e^{- \left(\frac{1 + \sqrt{1 + 4(1+\alpha)(J+N)}}{2(1+\alpha)} \right)}$$

$$B_7 = \frac{-(AB_4 z_6 \beta^* + 2\alpha B_3 \beta^*)}{(1+\alpha)\beta^{*2} + \beta^* - (J+N)}, \quad B_8 = \frac{(AB_5 z_1 + G_c B)}{(1+\alpha)z_1^2 + z_1 - (J+N)}, \quad B_{10} = \frac{(AB_5 z_2 + G_r B_2)}{(1+\alpha)z_2^2 + z_2 - (J+N)}, \quad B_9 = \frac{-G_c D_1 e^{z_2 y}}{(1+\alpha)z_2^2 + z_2 - (J+N)}$$

$$B_{11} = \frac{-Gr D_5}{(1+\alpha)z_3^2 + z_3 - (J+N)}, \quad B_{12} = \frac{2\alpha B_3 \beta^*}{(1+\alpha)z_3^2 + z_3 - (J+N)}, \quad B_{13} = \frac{-AD_{11} z_6}{(1+\alpha)z_6^2 + z_6 - (J+N)}$$

$$D_{13} = \frac{(AB_4 z_6 \beta^* + 2\alpha B_3 \beta^*)}{(1+\alpha)\beta^{*2} + \beta^* - (J+N)} - \frac{(AB_5 z_1 + G_c B)}{(1+\alpha)z_1^2 + z_1 - (J+N)} + \frac{G_c D_1}{(1+\alpha)z_2^2 + z_2 - (J+N)} - \frac{(AB_5 z_2 + G_r B_2)}{(1+\alpha)z_2^2 + z_2 - (J+N)} + \frac{Gr D_5}{(1+\alpha)z_3^2 + z_3 - (J+N)} - \frac{2\alpha B_3 \beta^*}{(1+\alpha)z_3^2 + z_3 - (J+N)} + \frac{AD_{11} z_6}{(1+\alpha)z_6^2 + z_6 - (J+N)}$$